Philosophical Magazine

ISSN: (Print) (Online) Journal homepage: https://www.tandfonline.com/loi/tphm20

Synergy of grain boundary and interface diffusion during intermediate compound formation

Andriy Gusak & Anastasiia Titova

To cite this article: Andriy Gusak & Anastasiia Titova (2023): Synergy of grain boundary and interface diffusion during intermediate compound formation, Philosophical Magazine, DOI: 10.1080/14786435.2023.2169381

To link to this article: https://doi.org/10.1080/14786435.2023.2169381

Published online: 03 Feb 2023.

PHILOSOPHICAL MAGAZINE
https://doi.org/10.1080/14786435.2023.2169381

Taylor & Francis
Taylor & Francis Group

Synergy of grain boundary and interface diffusion during intermediate compound formation

Andriy Gusak[a,b] and Anastasiia Titova[a]

[a]Ensemble3 Centre of Excellence, Warsaw, Poland; [b]Bohdan Khmelnytsky National University of Cherkasy, Cherkasy, Ukraine

ABSTRACT

The kinetics of reactive growth of a compound with a columnar structure with frozen bulk diffusion is revisited. The finite rate of redistribution and reaction along moving interfaces between reagents and growing compound is taken into account. Cases of planar and curved inter-phase interfaces are discussed. A new kinetic equation for the phase growth with evolving grain boundaries is suggested. Three cases are considered: (1) frozen grain structure, (2) normal lateral grain growth which does not depend on phase growth and on diffusion fluxes, (3) flux-driven grain growth which is induced by grain-boundary diffusion fluxes across the growing compound layer. The latter model provides the best fit to the experimental data.

ARTICLE HISTORY
Received 7 November 2022
Accepted 11 January 2023

KEYWORDS
Interdiffusion; intermediate compound; grain boundary diffusion; interface diffusion; grain growth; non-equilibrium thermodynamics

1. Introduction

Recently the formation kinetics of technologically important spinel $ZnAl_2O_4$ during the solid-state reaction between ZnO and amorphous Al_2O_3 was revisited [1]. The process is controlled mainly by interface diffusion (at the stage of nucleation and lateral growth) and later by the grain-boundary diffusion across the growing compound layer. In general, solid-state reactions in nanomaterials, or leading to the formation of nanomaterials, often proceed at comparatively low temperatures when the bulk diffusion is practically frozen, and all mass transport proceeds via grain boundaries or/and inter-phase interfaces. Often this transport proceeds simultaneously with the migration of these boundaries and interfaces (Cellular Precipitation – CP, Diffusion-Induced Grain-boundary Migration DIGM [2,3], Diffusion-Induced Recrystallisation, Cold Homogenisation [4–6]) and Liquid Film Migration (LFM). Close to such phenomena is a Flux-Driven Ripening of Cu_6Sn_5 scallops during soldering, when the scallops are growing and coarsening due to fast diffusion along moving liquid channels which appear due to wetting of grain-boundaries between grains of Cu_6Sn_5 by liquid tin and at

CONTACT Anastasiia Titova titova.anastasiya@vu.cdu.edu.ua

practically frozen bulk diffusion within scallops. [7–10]. Even more complicated combination of interface and surface diffusion with simultaneous formation of porous, sponge-like Cu_3Sn was discussed and modelled in [11]. Also, as suggested first in [12], the lateral grain growth may be induced by the deposition flux during the thin film deposition.

Here we consider the growth of intermediate phase with columnar structure under condition of frozen bulk diffusion. One of the first papers considering (experimentally and theoretically) a simultaneous phase and grain growth was the reference [13,14], in which the main process of the bronze technology for superconducting intermetallic Nb_3Sn formation in the solid-state reaction of Nb with binary alloy Cu-Sn was studied. The model of Gilmer-Farrell took into account the influence of lateral grain growth on the phase growth kinetics. Phase growth rate when bulk diffusion can be neglected is inversely proportional to the mean lateral grain size. Then, in the case of power-like time dependencies for mean lateral grain size $R = \kappa t^m$ and the phase layer growth kinetics $X = kt^n$ the exponents should be linked by the relation $m = 1-2n$. In fact, they found experimentally $m = 0.17 \pm 0.11$, $n = 0.35 \pm 0.06$. Later, a similar analysis was suggested by Ghosh [15].

In the previous papers, to the best of our knowledge, the diffusion along the interfaces between the growing columnar compound layer with reactants was not properly taken into account, and this simplification may significantly change the growth kinetics, and may be, the grain structure evolution. It can be seen in schematical Figure 1: atoms A migrating along grain-boundaries in A to react with B, spend part of their time for lateral diffusion before assembling at the 'left' triple junctions A/i, and also some time for more or less uniform redistribution and reaction with B reactant along the interface i/B.

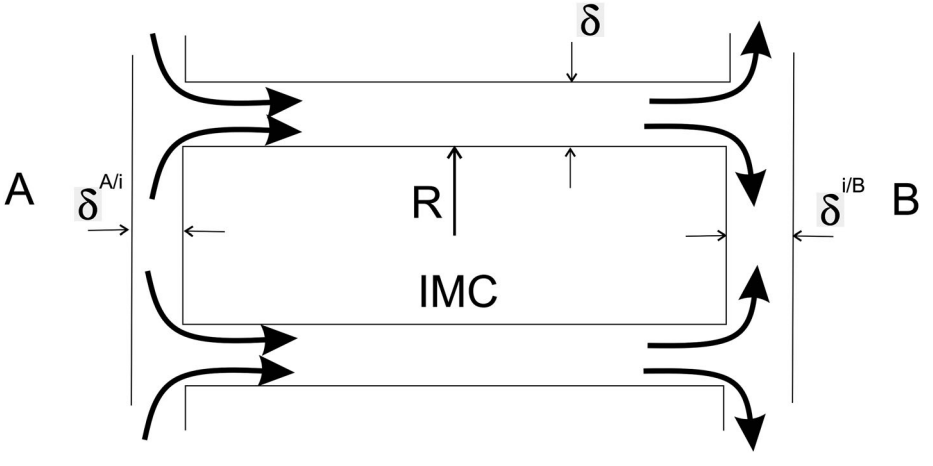

Figure 1. Intermediate phase formation by grain-boundary diffusion via grain boundaries with simultaneous interface diffusion when bulk diffusion is frozen.

This kinetics should be calculated and taken into account. (Of course, a similar problem exists with the flux of B-atoms migrating from B to react with A.) On the other hand, atoms A arriving along the GB within the compound to the 'right' triple junction i/B, may choose where to attach and, respectively what's grain increment to make wider after reaction with B in the new atomic layer of compound. We call such mechanism a 'Flux-induced grain growth' [12,16].

Namely, along with well-known normal grain growth in any cross-section perpendicular to the main diffusion flux, one more mechanism of grain growth becomes possible: even if the grain boundaries mobility with respect to normal lateral grain growth is close to zero, the grains may compete and grow at the expense of their neighbours (not uniformly, but only at the interphase boundaries), due to the redistribution of atoms arriving (along the grain boundaries) to the junctions of grain and interphase boundaries. At such junctions, any arriving atom should react and join the new monoatomic layer of one of two neighbouring grains (two sides of the grain boundary). The joining process is a choosing procedure, and the larger grain (due to larger radius of curvature and lower Gibbs-Thomson potential) has more chances to be chosen.

If the reaction stops, the normal grain growth may proceed further, but the flux-induced growth stops, since no material can be redistributed at the junctions. It means that at zero external fluxes such morphology evolution would be frozen. We call such type of morphology evolution in open systems – the 'flux-driven' processes. Here we would like to take into account both types of lateral grain growth – normal and flux-driven one.

In Section 2, we reconsider (in terms of Onsager formalism) the almost trivial model of monosize approximation of the columnar compound growth, with an account of only one controlling stage – longitudinal diffusion along the grain boundaries. In short Section 3, we improve the results of Section 2 by taking into account the Gibbs-Thomson capillary effect. In Section 4, we take into account the finite rate of two more stages of diffusion – lateral diffusion along the moving interfaces A/i and i/B. In Section 5 we introduce the lateral grain size distribution and various possibilities for grain growth during reactive diffusion. The synergy of phase growth and grain growth is analysed.

2. Monosize kinetic model of single compound growth controlled by grain-boundary diffusion

Results of this Section 2 are not new – we just introduce the necessary terms and remind the basic equations needed in the next Sections. Let the single phase with a very narrow homogeneity range grow between the two mutually insoluble components A and B.

Our picture of columnar structure is based on the mechanisms of phase formation, first experimentally found by Barmak et al [17] as a two-stage phase formation: The first stage is nucleation and DIGM-like spreading of nanometres-thick islands along the interface till the full covering is reached. Spreading was later modelled in [18–20]. Second stage starts after formation of continuous phase layer with grain-boundaries at the places of meeting of the spreading islands – it is a normal growth. Our model treats this second stage (normal growth) after formation of continuous layer of new phase.

We treat the case when the grain size in pure components is larger than in the AB intermetallic or of the same order of magnitude. The nuclei of intermediate phase emerge, most probably, at the triple joints of A/A or B/B grain-boundaries with A/B interface. After nucleation the spreading along contact interface is thermodynamically and kinetically more favourable than along the grain-boundaries within A/A or B/B. Thermodynamic favour of plate-like shape along interface in the sharp concentration gradient was proved in [21–23]. Kinetic favour of lateral spreading was demonstrated in [19,20]. Let us consider shortly some alternatives to this geometry, when the grains in pure components are smaller than in compound layer. In general, one might expect two sub-cases. In the first sub-case (small equiaxial grain of A or B or both), one may imagine some 'enveloping' of, say, small grains B by the fast grain-boundary diffusant A and forming initial core–shell structures (remnants of B-grains, covered by the nanolayers of compound) or the two-phase mixture of compound nano-grains with B-grains. Such evolution path will need another model.

The second sub-case corresponds to columnar structure not only of the compound but as well of at least one pure component. If the lateral size of B or A grains is smaller than the lateral size of AB-compound, the diffusion along interface will include the diffusion along or across the junctions of A/A or B/B grain-boundaries with interface – this case will be considered elsewhere.

Here we treat the phase growth after nucleation and lateral growth of nuclei, when the continuous phase layer has already been formed. The phase consists of cylindrical grains oriented along the concentration gradient. The mean lateral radius of grains will be further denoted as R. The total cross-section area (perpendicular to phase growth direction) is Area.

$$\text{Area} \cong \sum_{i=1}^{N} \pi R_i^2 = N\pi R^2 \tag{1}$$

(Of course, more rigorous treatment needs to consider a more realistic microstructure (i.e. honeycomb-like) instead of circular rods, but in grain-boundary diffusion problems such simplifications are usually considered as acceptable.)

Diffusion across the compound proceeds only via the longitudinal grain boundaries, with a total cross-section area of easy diffusion

$$A^{GB} = \sum_{i=1}^{N} 2\pi R_i \frac{\delta}{2} = \delta \sum_{i=1}^{N} \pi R_i = N\delta\pi R, \qquad \frac{A^{GB}}{Area} = \frac{\delta}{R}, \tag{2}$$

accompanied by lateral diffusive redistribution along the interfaces A/i and i/B. Atoms A are gathered to the thin (nanometric) grain-boundary channels of thickness 'δ' from the adjacent grains of material A, transported via grain-boundaries to the opposite interface i/B, are redistributed along this interface, and react with B. B-atoms do the same in the opposite direction. The difference in the partial grain-boundary diffusion of A and B is compensated by the Kirkendall shift of the whole lattice. A small modification of the Darken analysis [24] for interdiffusion via grain boundaries can be made using the total fluxes $I^{total} = A^{GB} \cdot j^{\|}$, where $j^{\|}$ is a flux density (number of atoms crossing unit cross-section) within the 'grain-boundary phase' along the grain boundaries of the columnar structure. The link between the partial grain-boundary fluxes and the Kirkendall velocity u of the total structure is given according, as usual, to Galileo's principle:

$$\Omega I_A^{total} = A^{GB}\Omega j_A^{\|} + \text{Area} \cdot c_A u, \qquad \Omega I_B^{total} = A^{GB}\Omega j_B^{\|} + \text{Area} \cdot c_B u \tag{3}$$

Here c_A, c_B are the atomic fractions of components within grain-boundaries ($c_A + c_B = 1$), Ω is a volume per atom, ΩI is the density of volume flux, measured in m/s. Equation (3) is written in the laboratory (Matano) reference frame – in this frame, the sum of fluxes should be zero: $\Omega I_A^{total} + \Omega I_B^{total} = 0$. Thus, $A^{GB}(\Omega j_A^{\|} + \Omega j_B^{\|}) + \text{Area} \cdot u = 0$, which immediately gives the drift velocity of the growing compound and the total fluxes:

$$u = -\frac{\delta}{R}(\Omega j_A^{\|} + \Omega j_B^{\|}) \tag{4}$$

$$\begin{aligned} \Omega I_A^{total} &= \text{Area} \cdot \left(\frac{\delta}{R}\Omega j_A^{\|} - c_A \frac{\delta}{R}(\Omega j_A^{\|} + \Omega j_B^{\|}) \right) \\ &= \text{Area} \cdot \frac{\delta}{R}(c_B \Omega j_A^{\|} - c_A \Omega j_B^{\|}) = -\Omega I_B^{total}. \end{aligned} \tag{5}$$

We write down here the partial fluxes in Onsager form, in terms of diffusion potential gradients, instead of the Fickian form of concentration gradient since concentration gradient within almost stoichiometric compounds is

difficult to measure:

$$\Omega j_A^{\parallel} = -L_A^{GB}\frac{\partial \mu_A}{\partial x} = +L_A^{GB} c_B \frac{\partial \tilde{\mu}}{\partial x},$$

$$\Omega j_B^{\parallel} = -L_B^{GB}\frac{\partial \mu_B}{\partial x} = -L_B^{GB} c_A \frac{\partial \tilde{\mu}}{\partial x} = -\frac{D_B^{*GB}}{D_A^{*GB}} L_A^{GB} c_B \frac{\partial \tilde{\mu}}{\partial x} = -\frac{D_B^{*GB}}{D_A^{*GB}} \Omega j_A^{\parallel} \quad (6)$$

Here $\tilde{\mu} \equiv \mu_B - \mu_A = \frac{\partial g}{\partial c_B}$ is a diffusion potential (change of Gibbs free energy due to the replacement of the A atom by the B atom). We also used the Gibbs-Duhem relation for the isothermic isobaric case: $c_A d\mu_A + c_B d\mu_B = 0$. Onsager coefficients are: $L_A^{GB} = \frac{c_A D_A^{*GB}}{kT}$, $L_B^{GB} = \frac{c_B D_B^{*GB}}{kT}$. (Here D_A^{*GB}, D_B^{*GB} are the tracer diffusivities within grain-boundaries.) Simple algebra then gives

$$\Omega I_B = -A\frac{\delta}{R}(c_A^2 L_B^{GB} + c_B^2 L_A^{GB})\frac{\partial \tilde{\mu}}{\partial x} = -A\frac{\delta}{R}\tilde{L}^{GB}\frac{\partial \tilde{\mu}}{\partial x} \quad (7)$$

Here the interdiffusion Onsager coefficient is

$$\tilde{L}^{GB} = c_A^2 L_B^{GB} + c_B^2 L_A^{GB} \quad (8)$$

Obviously, this expression is easily converted into Darken-type formula:

$$\Omega I_B = -A\frac{\delta}{R}(c_A D_B^{*GB} + c_B D_A^{*GB})\frac{c_A c_B}{kT}\frac{\partial \tilde{\mu}}{\partial x} \quad (9)$$

Here $\frac{\partial \tilde{\mu}}{\partial x} = \frac{\partial \tilde{\mu}}{\partial c_B}\frac{\partial c_B}{\partial x} = \frac{\partial^2 g}{\partial c_B^2}\frac{\partial c_B}{\partial x}$, $\varphi \equiv \frac{c_A c_B}{kT}\frac{\partial^2 g}{\partial c_B^2}$ – standard thermodynamic factor, so that

$$\Omega I_B = -A\frac{\delta}{R}(c_A D_B^{*GB} + c_B D_A^{*GB})\varphi\frac{\partial c_B}{\partial x}. \quad (10)$$

The just shown derivation of Darken-like Equations (4) and (10) for the case of 'pure' grain-boundary diffusion and frozen bulk diffusion seems mathematically trivial but our preliminary discussions demonstrated that the more 'physical' analysis and interpretation may be useful for better understanding. Most of models treating INTER-diffusion with account of grain boundaries, are concentrated on the B-regime of Harrison classification (or Fisher model in simple case of only one diffusant) when both grain-boundary diffusion and bulk diffusion (from grain-boundaries into grains) are important (see, for example [25,26,6]). One of the present authors (AG) published a paper on simultaneous grain-boundary and bulk diffusion with different grain-boundary diffusivities and different bulk diffusivities within grains in the model of spherical grains in the multigrain diffusion couple. The marker velocities appeared proportional to the difference of BULK diffusivities multiplied by some combination (but not difference) of grain-boundary diffusivities [27].

In case of diffusion of A from A to semi-infinite bi-crystal B along the grain-boundary under frozen bulk diffusivities an interesting model was suggested by Klinger and Rabkin [28]. They demonstrated that the difference of the grain boundary diffusivities leads to plating out of additional material at the grain boundary in the form of a wedge of extra material, which generates an elastic stress field in the vicinity of the grain boundary. Yet, in their case the problem had an important constraint which, luckily, we don't have in our problem – The 'extra'atoms going into the GB, had no 'way out'. In the conditions of phase layer growth due to grain-boundary diffusion along the columnar grains the extra atoms DO HAVE THE WAY OUT at the 'ends' of columns.

To simplify the picture, let us start with growth of almost stoichiometric equiatomic compound AB due to grain-boundary diffusion of only one component A with intrinsic diffusivity D_A from A to B. ($D_B = 0$). Let also the volume per atom in A-phase, B-phase and AB-phase is the same. Let dN_A atoms of sort A, which formed a layer of the thickness $dX = \Omega \frac{dN_A}{Area}$ (where Area is a total cross-section area), passed from A-side to the interface AB/B and reacted (during lateral spreading) with $dN_B = dN_A$ atoms of sort B. Together they formed a new layer at the 'right-hand side' of the thickness $2dX = \Omega \frac{dN_A + dN_B}{Area} = 2\Omega \frac{dN_A}{Area}$. Space 2dX for the new-formed layer of compound is provided by (1) interval dX of atoms B used for reaction, and (2) by the shift of whole grain also by dX to the 'left' filling the empty space dX left by the dN_A atoms which travelled via grain-boundaries to react with B. Of course, the same may be explained in terms of vacancy grain-boundary flux created by flux A and going to A and providing elimination of layer dX at the A-side and letting the whole grain to demonstrate the Kirkendall shift. Thus, vacanies dont need to find sinks/sources at the grain-boundaries or in the bulk. Vacancy sinks at the A/AB interface and vacancy sources at AB/B interface are sufficient.

Kirkendall velocity of the grain as whole is $u = -\frac{dX}{dt}$ (in our case grain as a whole moves left, from B to A (fast diffusant)). Obviously,

$$dX = \Omega \frac{dN_A}{Area}.$$

$$dN_A = j_A^{GB} \cdot A^{GB} \cdot dt.$$

$$\text{So, } u = -\Omega j_A^{GB} \frac{A^{GB}}{Area} \frac{dt}{dt} = -\Omega j_A^{GB} \frac{\delta}{R}.$$

This equation coincides with Equation (4) for the case when only A diffuses within GB.

Similar logic may explain the more general case of reaction $mA + nB = A_mB_n$ and for non-zero D_B. Here one can see some non-locality of Kirkendall shift and of the whole interdiffusion process: the Kirkendall shift at some plane is determined by the concentration gradient times difference of intrinsic diffusivities integrated over some interval related to migration length of vacancies. This peculiarity was noticed and proved for the case of interdiffusion in solid solution with non-ideal vacancy sources in 1985 [29]. In short, if the growing phase has columnar structure and bulk diffusion is frozen, each grain can be regarded as a Kirkendall marker!

Flux balance at moving interfaces A/i and i/B gives:

$$A(c_{iL} - 0)\frac{dx_{Ai}}{dt} = \Omega I_{BL} - 0, \qquad A(1 - c_{iR})\frac{dx_{iB}}{dt} = 0 - \Omega I_{BR} \tag{11}$$

We treat only the case of almost stoichiometric compounds with narrow concentration range, $\Delta c_i \equiv c_{iR} - c_{iL} \ll 1$. In this case, the steady-state approximation is valid for the flux [30], which is of course changing with time but remains the same near interfaces and inside the phase layer: $I_{BL} = I_{BR} = I_B$. For the phase thickness $\Delta x = x_{iB} - x_{Ai}$

$$\frac{d\Delta x}{dt} = \frac{1}{c_i(1-c_i)}\left(-\frac{\Omega I_B}{A}\right), \qquad \frac{d\Delta x}{dt} = \frac{1}{c_i(1-c_i)}\frac{\delta}{R}\tilde{L}^{GB}\frac{\Delta\tilde{\mu}^{\parallel}}{\Delta x}. \tag{12}$$

Here the driving force of interdiffusion can be calculated with an account of

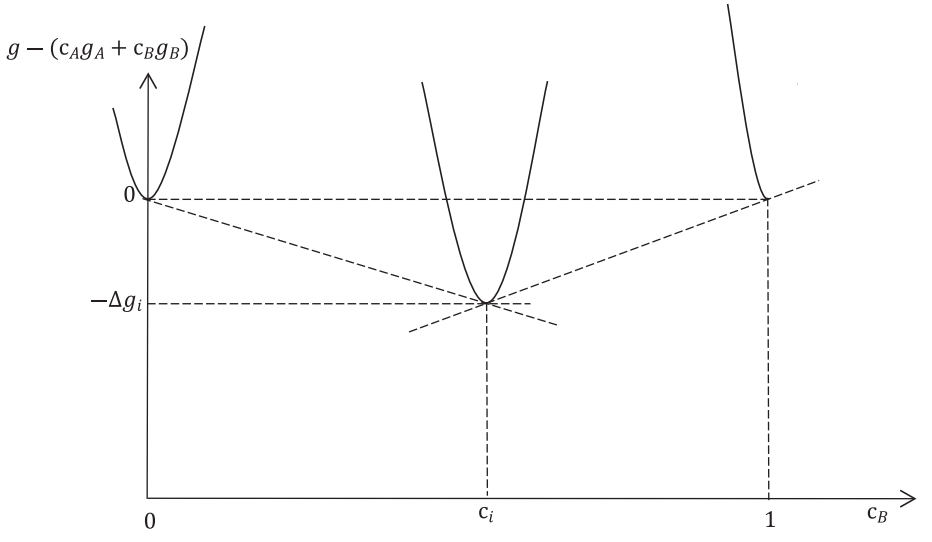

Figure 2. Schematic g-curves and common tangent construction for calculation of the thermodynamic driving force.

common tangent construction (Figure 2)

$$\Delta\tilde{\mu}^{\|} = \frac{\partial g}{\partial c_B}|_{i/B} - \frac{\partial g}{\partial c_B}|_{A/i} \approx \frac{0-(-\Delta g_i)}{1-c_i} - \frac{(-\Delta g_i)-0}{c_i-0} = \frac{\Delta g_i}{c_i(1-c_i)} \tag{13}$$

Thus, the growth kinetics under the assumption of very fast lateral redistribution at the moving interfaces satisfies the following law:

$$\frac{d\Delta x}{dt} = \frac{1}{c_i^2(1-c_i)^2}\frac{\delta}{R}\frac{\tilde{L}^{GB}\Delta g_i}{\Delta x}. \tag{14}$$

3. Taking into account the capillary effect

Let us check the validity of expression (14) with the assistance of thermodynamic analysis. Namely, let us, as typical for non-equilibrium thermodynamic analysis [31,32], equalise the Gibbs free energy release rate during reactive diffusion, $-\frac{dG}{dt}$, and the total entropy production in local relaxation processes, times temperature, $T\frac{dS}{dt}$.

For the case of single-phase growth controlled by grain-boundary diffusion via columnar grain structure when (1) bulk diffusion and lateral grain growth are frozen, and (2) lateral diffusion along interfaces A/I and I/B is infinitely fast, one gets

$$\Delta G = -\Delta g_i \frac{(\text{Area}\cdot\Delta x)}{\Omega} + \sum_i \gamma l_i \Delta x, \tag{15}$$

$$\left(\sum \text{over all arcs}\right), \text{sum of all } l_i = \text{const} \left(\text{no grain growth in this Section is considered}\right)$$

$$-\frac{d\Delta G}{dt} = \frac{g_1}{\Omega}\text{Area}\frac{d\Delta x}{dt} - \gamma\sum_i l_i\frac{d\Delta x}{dt} = \frac{\text{Area}}{\Omega}\left\{\Delta g_i - \gamma\frac{\sum_i l_i}{A}\right\}\frac{d\Delta x}{dt}, \tag{16}$$

$$T\frac{dS}{dt} = \left(\sum_i l_i\delta\Delta x\right)\frac{\tilde{L}^{GB}}{\Omega}\left(\frac{\Delta\mu}{\Delta x}\right)^2 \tag{17}$$

Here $\sum_i l_i\delta\Delta x$ is (within columnar structure mode) a volume of grain-boundary^{i}diffusion,

$$\frac{d\Delta x}{dt} = \frac{-\Omega J_i}{\text{Area}*c_i(1-c_i)} = \frac{\sum_i l_i\delta\Delta\tilde{L}^{GB}\frac{\Delta\mu}{\Delta x}}{\text{Area}*c_i(1-c_i)}. \tag{18}$$

Comparing the expressions (16) and (17) while taking into account Equation (18), one gets

$$\frac{Area}{\Omega}\Delta g_i\left\{1-\gamma\Omega\frac{\sum_i l_i}{\text{Area}*\Delta g_i}\right\}\cdot\frac{\sum_i l_i\delta\Delta\tilde{L}^{GB}}{\text{Area}*c_i(1-c_i)}\frac{\Delta\mu}{\Delta x}$$
$$=\left(\sum_i l_i\delta\right)\Delta x\frac{\tilde{L}^{GB}}{\Omega}\left(\frac{\Delta\mu}{\Delta x}\right)^2. \tag{19}$$

$$\Delta\mu=\frac{\Delta g_i}{c_1(1-c_1)}\left\{1--\frac{\gamma\Omega}{g_1}\frac{\sum_i l_i}{\text{Area}}\right\}$$

In the simplified model of cylindrical grains (rods):

$$\text{Area}=\sum_k\pi R_k^2,\qquad\sum_i l_i=\frac{1}{2}\sum_k 2\pi R_k$$

$$\frac{\frac{1}{2}\sum_k 2\pi R_k}{\sum_k\pi R_k^2}=\frac{\sum_k R_k}{\sum_k R_k^2}=\frac{\langle R\rangle}{\langle R^2\rangle}\equiv\frac{1}{\rho},\ \text{so that}\qquad\frac{\sum_i l_i\delta}{\text{Area}}=\frac{\langle R\rangle}{\langle R^2\rangle}\delta. \tag{20}$$

Then

$$\Delta\mu=\frac{\Delta g_i}{c_1(1-c_1)}\left\{1-\frac{\gamma\Omega/\rho}{\Delta g_i}\right\}=\frac{\Delta g_i}{c_1(1-c_1)}\left\{1-\frac{\rho_{cr}}{\rho}\right\} \tag{21}$$

Under the condition $\rho<\rho_{cr}=\dfrac{\gamma\Omega}{\Delta g_i}$, the reaction should stop.

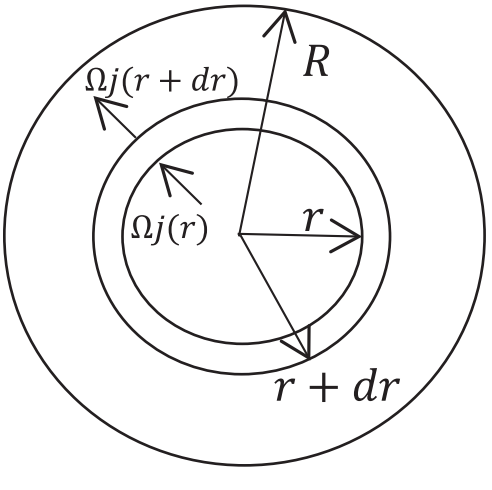

Figure 3. Quasi-steady-state lateral diffusion along interface i/B.

Thus, Equations (14) for monosize model should be also modified:

$$\frac{d\Delta x}{dt} = \frac{1}{c_i^2(1-c_i)^2}\frac{\delta}{R}\frac{\tilde{L}^{GB}(\Delta g_i - \gamma\Omega/\mathrm{R})}{\Delta x} \tag{22}$$

The same result could be obtained directly within common tangents construction in Figure 3 and Equation (13) if one takes the Gibbs-Thomson potential into account and substitutes the driving force $-\Delta g_i$ by $-\Delta g_i + \gamma\Omega/\mathrm{R}$.

4. Taking into account lateral fluxes along interfaces in the framework of the monosize model

Consider now the diffusion and reaction processes at the moving interface i/B with δ_{iB}^{int} in the reference frame of this very interface. In this reference frame, the interface is immobile, and the interface moves from reagent B inside, changing concentration c_i into 1. In the steady-state approximation the conservation condition for B atoms within the narrow circular shell of thickness dR and width δ_{iB}^{int} gives:

$$\mathrm{dt}\cdot\delta_{iB}^{int}[\Omega j_B^{\perp}(\mathrm{r})\cdot 2\pi\mathrm{r} - \Omega j_B^{\perp}(\mathrm{r}+\mathrm{dr})\cdot 2\pi(\mathrm{r}+\mathrm{dr})] + (1-\mathrm{c_i})\mathrm{dx_{iB}}\cdot 2\pi\mathrm{rdr} = 0, \tag{23}$$

The last term in the left-hand side of Equation (23). $\mathrm{dx_{iB}}\cdot\frac{2\pi\mathrm{rdr}}{\Omega}$ is a number of B-atoms, which belonged to the layer $\mathrm{dx_{iB}}$ before reaction. $\mathrm{c_i}$ is a fraction of B in the just-formed compound, so that $\mathrm{c_i}\cdot\mathrm{dx_{iB}}\cdot\frac{2\pi\mathrm{rdr}}{\Omega}$ is a number of B-atoms in the same layer AFTER the reaction, or, in other words, it is a number of atoms 'lost to A + B = AB reaction'. The rest, $(1-\mathrm{c_i})\cdot\mathrm{dx_{iB}}\cdot\frac{2\pi\mathrm{rdr}}{\Omega}$, is a number of atoms B which did not react with A at the interface AB/B, and instead started to migrate towards A/AB interface to react with A at that interface. Equivalently, one may say that $(1-\mathrm{c_i})\cdot\mathrm{dx_{iB}}\cdot\frac{2\pi\mathrm{rdr}}{\Omega}$ is a number of atoms A, which came from interface A/AB to react with $\mathrm{c_i}\cdot\mathrm{dx_{iB}}\cdot\frac{2\pi\mathrm{rdr}}{\Omega}$ atoms B to form a layer of compound $A_{1-ci}B_{ci}$ of thickness $\mathrm{dx_{iB}}$. The rest of B (number of atoms B which did not react with A at AB/B interface), determines the divergence of lateral flux B along the AB/B interface – and it corresponds to the first two terms in the left-hand side of Equation (23) From Equation (23) one easily

gets:

$$\Omega j_B^{\perp}(r) = \frac{1 - c_i}{2\delta_{iB}^{int}} \frac{dx_{iB}}{dt} \cdot r \tag{24}$$

$$\Omega j_B^{\perp}(R) = \frac{1 - c_i}{2\delta_{iB}^{int}} \frac{dx_{iB}}{dt} \cdot R \tag{25}$$

Continuity of total flux when it converts from longitudinal along grain boundaries into lateral flux along the interface i/B means: $-2\pi R \frac{\delta^{GB}}{2} \Omega j_B^{\parallel} = 2\pi R \delta_{iB}^{int} \cdot \Omega j_B^{\perp}(R)$. It gives

$$\frac{1 - c_i}{2} \frac{dx_{iB}}{dt} R = -\frac{\delta^{GB}}{2} \Omega j_B^{\parallel} = +\frac{\delta^{GB}}{2} \tilde{L}^{GB} \frac{\Delta \tilde{\mu}^{\parallel}}{\Delta x}, \text{ so that}$$

$$\frac{dx_{iB}}{dt} = \frac{1}{1 - c_i} \frac{\delta^{GB}}{R} \tilde{L}^{GB} \frac{\Delta \tilde{\mu}^{\parallel}}{\Delta x}. \tag{26}$$

Now the diffusion potential changes not only at the grain boundaries (this change we denote as $\Delta\tilde{\mu}^{\parallel}$) but along the interphase interfaces as well. Namely,

$$\Omega j_B(r) = -\tilde{L}_{iB}^{int} \frac{\partial \tilde{\mu}}{\partial r}. \tag{27}$$

$$\frac{d\ddot{A}}{dr} = \frac{1 - c_i}{2\tilde{L}_{iB}^{int}\delta_{iB}^{int}} \frac{dx_{iB}}{dt} \cdot r \tag{28}$$

Thus, the diffusion potential increments at the interface i/B and, by analogy, at the interface A/i, can be found:

$$\Delta\tilde{\mu}_{iB} \equiv \tilde{\mu}_{iB}(0) - \tilde{\mu}_{iB}(R) = \frac{1 - c_i}{4\tilde{L}_{iB}^{int}\delta_{iB}^{int}} \frac{dx_{iB}}{dt} \cdot R^2, \tag{29b}$$

$$\Delta\tilde{\mu}_{Ai} \equiv \tilde{\mu}_{Ai}(0) - \tilde{\mu}_{Ai}(R) = \frac{1 - c_i}{4\tilde{L}_{Ai}^{int}\delta_{Ai}^{int}} \frac{dx_{Ai}}{dt} \cdot R^2. \tag{29a}$$

Substituting equations (11, 12) for the interface velocities, one gets the links between the interface steps of diffusion potential and the change of diffusion potential along the grain boundaries:

$$\Delta\tilde{\mu}_{iB} = \frac{1 - c_i}{4\tilde{L}_{iB}^{int}\delta_{iB}^{int}} \cdot R^2 \cdot \frac{1}{1 - c_i} \frac{\delta^{GB}}{R} \tilde{L}^{GB} \frac{\Delta\tilde{\mu}^{\parallel}}{\Delta x} = \frac{R}{4\Delta x} \left(\frac{\delta^{GB}}{\delta_{iB}^{int}}\right) \left(\frac{\tilde{L}^{GB}}{\tilde{L}_{iB}^{int}}\right) \Delta\tilde{\mu}^{\parallel} \tag{30b}$$

$$\Delta\tilde{\mu}_{Ai} = \frac{1 - c_i}{4\tilde{L}_{Ai}^{int}\delta_{Ai}^{int}} \cdot R^2 \cdot \frac{1}{1 - c_i} \frac{\delta^{GB}}{R} \tilde{L}^{GB} \frac{\Delta\tilde{\mu}^{\parallel}}{\Delta x} = \frac{R}{4\Delta x} \left(\frac{\delta^{GB}}{\delta_{Ai}^{int}}\right) \left(\frac{\tilde{L}^{GB}}{\tilde{L}_{Ai}^{int}}\right) \Delta\tilde{\mu}^{\parallel} \tag{30a}$$

The total change, of course, should be the same as in Equation (13) with modification

concerning Gibbs-Thomson potential:

$$\Delta\tilde{\mu}_{\mathrm{Ai}} + \Delta\tilde{\mu}^{\parallel} + \Delta\tilde{\mu}_{\mathrm{iB}} = \frac{\Delta g_{\mathrm{i}}}{c_{\mathrm{i}}(1-c_{\mathrm{i}})}\left(1 - \frac{\gamma\Omega/R}{\Delta g_i}\right). \tag{31}$$

Substitution of Equation (30) into Equation (31) gives:

$$\Delta\mu^{\parallel}\left\{1 + p\frac{R}{4\Delta x}\right\} = \frac{\Delta g_{\mathrm{i}}\left(1 - \frac{\gamma\Omega/R}{\Delta g_i}\right)}{c_{\mathrm{i}}(1-c_{\mathrm{i}})},\ p \equiv \frac{1}{4}\delta^{GB}\tilde{L}^{GB}\left[\frac{1}{\delta^{\mathrm{int}}_{\mathrm{Ai}}\tilde{L}^{\mathrm{int}}_{\mathrm{Ai}}} + \frac{1}{\delta^{\mathrm{int}}_{\mathrm{iB}}\tilde{L}^{\mathrm{int}}_{\mathrm{iB}}}\right], \tag{32}$$

so that

$$\Delta\tilde{\mu}^{\parallel} = \frac{\Delta g_i\left(1 - \frac{\gamma\Omega/R}{\Delta g_i}\right)}{c_i^2(1-c_i)^2\left[1 + p\frac{R}{\Delta x}\right]}, \tag{33}$$

$$\frac{d\Delta x}{dt} = \frac{\tilde{L}^{GB}}{c_i^2(1-c_i)^2}\frac{\delta}{R}\cdot\frac{\Delta g_i - \frac{\gamma\Omega}{R}}{\Delta x + pR} \tag{34}$$

To the best of our knowledge, Equation (34) was never obtained before. One may interpret the denominator in this equation as some integral effective distance that should be travelled by atoms to complete the reactions – this distance includes the layer thickness as well as lateral size of the grain (with some coefficient, depending on the ratio of diffusivities along the grain- and interphase boundaries).

Modifications of Equation (34) due to dispersion of grain radii (lateral grain sizes) and due to curved interfaces are derived in Appendix A1.

5. Normal and flux-driven grain growth during phase layer growth

Equation (34) contains two time-dependent variables – phase thickness and lateral grain radius. In the realistic case of some distribution of lateral sizes, it should be mean radius or mean squared radius. Measuring grain size distribution in the compound layers with columnar structure and especially the time evolution of this distribution, as well as the possible gradients of lateral grain sizes still remains a challenge for experimental researchers. In a very idealistic case of zero solute drag, etc., one could assume a parabolic growth law for mean radius. In previous models with $p = 0$ and $R_{cr} \to 0$ in the Equation (34) substitution of R proportional to the square root of time immediately led to the power law with exponent 0.25 for the compound thickness. It is rather far from the majority of experimental data – they are roughly between 0.33 and

0.5, and most interesting for our papers [15,1] they coincide and are equal to about 0.37.

Let us consider three cases of Equation (34).

Case 1. Mean size R is almost constant, lateral grain growth is locked by solute drag at grain boundaries or by any other factor. In this case, Equation (34) gives the linear-parabolic dependence:

$$\text{linear}\ , \quad \Delta x \cong \frac{\tilde{L}^{GB}}{c_i^2(1-c_i)^2}\frac{\delta}{R}\cdot\frac{\Delta g_i\left(1-\dfrac{\gamma\Omega/\mathrm{R}}{\Delta g_i}\right)}{pR}\times \mathrm{t} \quad \text{at } \Delta x << pR, \text{ and} \quad (35a)$$

$$\text{parabolic}, \quad (\Delta x)^2 \cong \frac{2\tilde{L}^{GB}}{c_i^2(1-c_i)^2}\frac{\delta}{R}\cdot\left(\Delta g_i-\frac{\gamma\Omega}{R}\right)\times \mathrm{t}\ , \quad \text{at } \Delta x >> pR\ . \quad (35b)$$

Case 2. If one assumes that the mean lateral grain size satisfies the parabolic law (typical for pure grain growth without solute drag), $R(t)=\sqrt{R_0^2+kt}$, where R_0^2 is the mean squared lateral size of initial nuclei of the forming phase at the moment of continuous layer formation, then the phase thickness has rather complicated growth law with exponent changing with phase thickness. A typical numeric solution for the time-dependent growth exponent $\mathrm{n}=\dfrac{\mathrm{dln}\Delta\mathrm{x}}{\mathrm{dlnt}}$ is shown in Figure 4.

Case 3 (Figure 5). So far, during the longitudinal growth of columnar grains the cross-section of each grain is reproduced in each new atomic layer formed due to

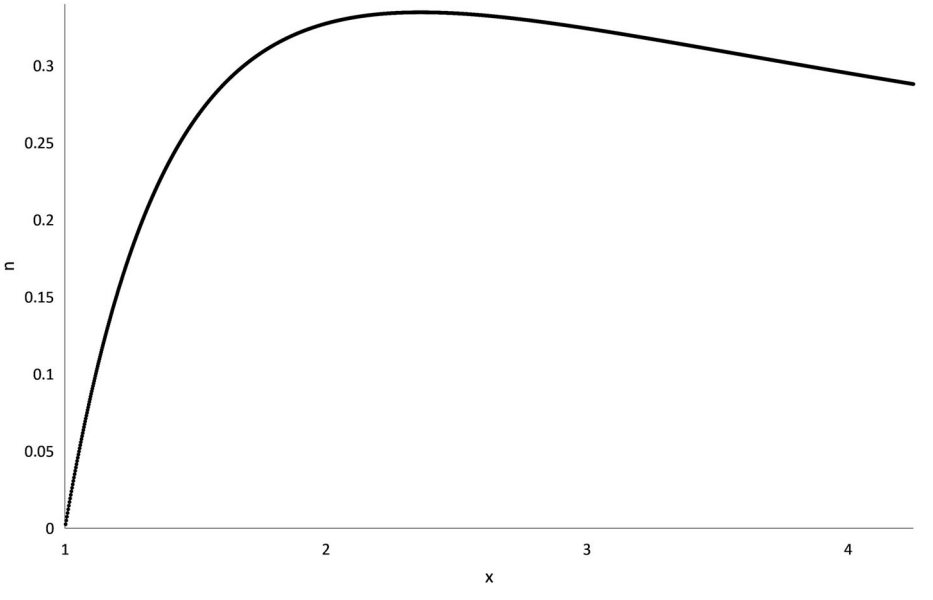

Figure 4. Typical numeric solution of Equation (34) in the case 2, when $R(t)=\sqrt{R_0^2+kt}$. Abscissa corresponds to reduced phase thickness $\dfrac{\Delta x}{\Delta x_0}$ (Δx_0 - initial phase thickness), after formation of continuous layer, typically up to 10 nanometres.

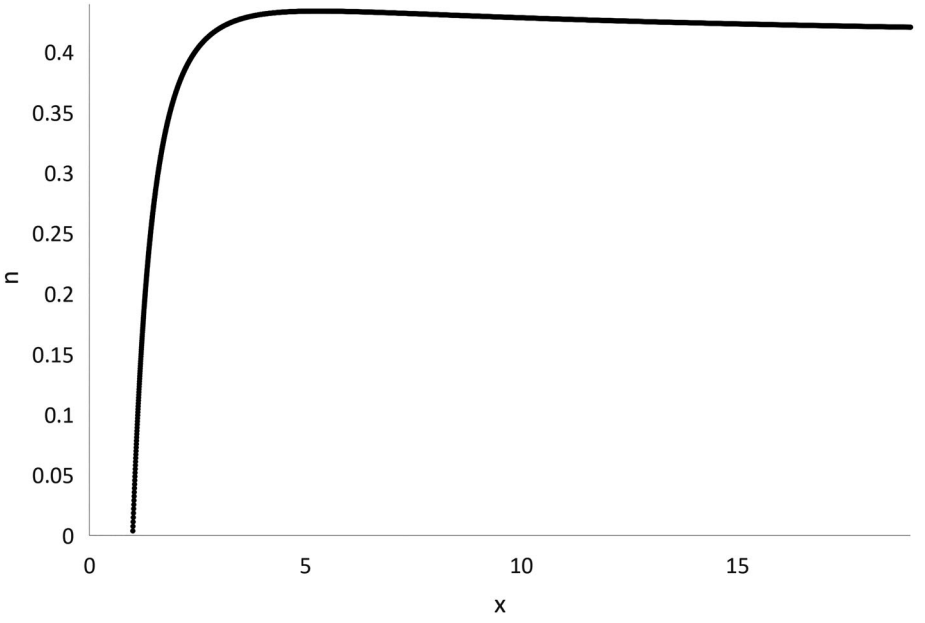

Figure 5. Case 3 of the flux-driven grain growth. Typical dependence of power exponent $n = \frac{d\ln\Delta x}{d\ln t}$ for phase growth around 0.4 (for grain size, according to Equation (36), it will be divided by 2 – about 0.20 due to square root in Equation (36)). The power exponents 0.4 and 0.2 are close to the experimental results of [1] and [15].

the reaction of incoming A-flux with species B at the interface compound/reagent B. (And analogically with B atoms coming to form the new atomic layer of the compound at A/i interface.) Yet, in reality, the physical picture may be even more complicated [15]. Namely, at each new growth step – during the formation of a new atomic layer the grain bottom (or grain top) becomes a bit wider or thinner. It proceeds due to the same capillary driving forces but the mechanism is different: in normal grain growth, the atoms should leave one grain and immediately join another one. In our case of the flux-driven grain growth, the atoms do not need to leave any grain – they are already migrating within GB-subsystem. All that they should do – is to choose what grain to join during the formation of the new atomic layer of this grain. This additional choice makes larger grains a bit larger, and smaller grains – a bit smaller. In ref.[16] we demonstrated that under some natural assumptions, during such flux-driven grain growth the radius of grain should change with thickness according to

$$\frac{dR}{d\Delta x} \sim \sqrt{\alpha/R} = \sqrt{\frac{\gamma\Omega}{kTR}}, \text{ so that } R \sim \sqrt{\alpha\Delta x}. \tag{36}$$

Thus, in case 3 one gets,
$$\frac{d\Delta x}{dt} = \frac{\tilde{L}^{GB}}{c_i^2(1-c_i)^2}\frac{\delta}{\sqrt{\alpha\Delta x}} \cdot \frac{\Delta g_i\left(1-\frac{\gamma\Omega/\sqrt{\alpha\Delta x}}{\Delta g_i}\right)}{\Delta x + p\sqrt{\alpha\Delta x}} \tag{37}$$

6. Summary

New kinetic Equation (34) for the reactive growth of compound with columnar grain structure is derived, taking into account the redistribution kinetics of atoms along interfaces compound/reagent, as well as simultaneous grain and phase growth. At least in some cases, better agreement with experimentally observed kinetics is obtained for the flux-driven grain growth (power exponents close to 0.4 for phase thickness, and 0.2 for lateral grain size).

Acknowledgements

Authors are grateful to Prof. K.N.Tu, Dr. Cs. Cserhati and to Prof. D.A.Pawlak for fruitful discussions.

Disclosure statement

No potential conflict of interest was reported by the author(s).

Funding

The authors thank the ENSEMBLE3 Project (MAB/2020/14) which is carried out within the International Research Agendas Programme (IRAP) of the Foundation for Polish Science (Fundacja na rzecz Nauki Polskiej) co-financed by the European Union under the European Regional Development Fund and the Teaming Horizon 2020 programme [GA #857543] of the European Commission.

References

[1] G. Jáger, J.J. Tomán, L. Juhász, G. Vecsei, Z. Erdélyi and C. Cserháti, *Nucleation and growth kinetics of $ZnAl_2O_4$ spinel in crystalline ZnO–amorphous Al_2O_3 bilayers prepared by atomic layer deposition*. Scr. Mater. 219 (2022 Oct 1), pp. 114857. doi:10.1016/j.scriptamat.2022.114857.

[2] N. Kaur, C. Deng and O.A. Ojo, *Effect of solute segregation on diffusion induced grain boundary migration studied by molecular dynamics simulations*. Comput. Mater. Sci. 179 (2020), pp. 109685. doi:10.1016/j.commatsci.2020.109685.

[3] E. Rabkin, *Gradient and coherency strain energies as driving forces for DIGM*. Scr. Metall. Mater. 30(11) (1994 Jun), pp. 1443–1448.
[4] N. Gazit, L. Klinger, G. Richter and E. Rabkin, *Formation of hollow gold-silver nanoparticles through the surface diffusion induced bulk intermixing*. Acta Mater. 117 (2016), pp. 188–196. doi:10.1016/j.actamat.2016.07.009.
[5] Y. Geguzin, *Cold' homogenization during interdiffusion in dispersed media*. Fiz. Met. Metalloved 54(1) (1982), pp. 137–143.
[6] D.L. Beke, Y. Kaganovskii and G.L. Katona, *Interdiffusion along grain boundaries – diffusion induced grain boundary migration, low temperature homogenization and reactions in nanostructured thin films*. Prog. Mater. Sci. 98 (2018), pp. 625–674. doi:10.1016/j.pmatsci.2018.07.001.
[7] A.M. Gusak and K.N. Tu, *Kinetic theory of flux-driven ripening*. Physical Review B 66 (11) (2002), pp. 115403. doi:10.1103/PhysRevB.66.115403.
[8] K.N. Tu, A.M. Gusak and M. Li, *Physics and materials challenges for lead-free solders*. J. Appl. Phys. (2003 Feb 1). doi:10.1063/1.1517165
[9] J.O. Suh, K.N. Tu, G.V. Lutsenko and A.M. Gusak, *Size distribution and morphology of Cu6Sn5 scallops in wetting reaction between molten solder and copper*. Acta Mater. (2008 Mar 1). doi:10.1016/j.actamat.2007.11.009
[10] A.M. Gusak, K.N. Tu and C. Chen, *Extremely rapid grain growth in scallop-type Cu6Sn5 during solid–liquid interdiffusion reactions in micro-bump solder joints*. Scr. Mater. 179 (2020), pp. 45–48. doi:10.1016/j.scriptamat.2020.01.005.
[11] A.M. Gusak, C. Chen and K.N. Tu, *Flux-driven cellular precipitation in open system to form porous Cu3Sn*. Philos. Mag. 96(13) (2016), pp. 1318–1331. doi:10.1080/14786435.2016.1162913.
[12] K.N. Tu, A.M. Gusak and I. Sobchenko, *Linear rate of grain growth in thin films during deposition*. Phys. Rev. B (2003 Jun 10). doi:10.1103/PhysRevB.67.245408
[13] H.H. Farrell, G.H. Gilmer and M. Suenaga, *Grain boundary diffusion and growth of intermetallic layers: Nb3Sn*. J. Appl. Phys. 45(9) (1974 Sep), pp. 4025–4035. doi:10.1063/1.1663907.
[14] G.H. Gilmer and H.H. Farrell, *Grain-boundary diffusion in thin films. II. Multiple grain boundaries and surface diffusion*. J. Appl. Phys. 47(10) (1976 Oct), pp. 4373–4380. doi:10.1063/1.322441.
[15] G. Ghosh, *Interfacial microstructure and the kinetics of interfacial reaction in diffusion couples between Sn–Pb solder and Cu/Ni/Pd metallization*. Acta Mater. 48(14) (2000 Sep 4), pp. 3719–3738. doi:10.1016/S1359-6454(00)00165-8.
[16] A.M. Gusak, *Flux-driven lateral grain growth during reactive diffusion*. Metallofiz. Noveishie Tekhnol 42(10) (2020), pp. 1335–1346. doi:10.15407/mfint.42.10.1335.
[17] C. Michaelsen, K. Barmak and T.P. Weihs, *Investigating the thermodynamics and kinetics of thin film reactions by differential scanning calorimetry*. J. Phys. D: Appl. Phys. 30(23) (1997), pp. 3167). doi:10.1088/0022-3727/30/23/001.
[18] L. Klinger, Y. Brechet and G. Purdy, *On the kinetics of interface-diffusion-controlled peritectoid reactions*. Acta Mater. 46(8) (1998), pp. 2617–2621. doi:10.1016/S1359-6454(97)00471-0.
[19] G. Lucenko and A. Gusak, *A model of the growth of intermediate phase islands in multilayers*. Microelectron. Eng. 70(2–4) (2003), pp. 529–532. doi:10.1016/S0167-9317(03)00432-5.
[20] M. Pasichnyy and A. Gusak, *Model of lateral growth stage during reactive phase formation*, in *Defect and Diffusion Forum*, Trans Tech Publications Ltd, 2008, Vol. 277, pp. 47–52. doi:10.4028/www.scientific.net/DDF.277.47

[21] A.M. Gusak, O.V. Dubiy and S.V. Kornienko, *Nucleation of intermediate phases upon interdiffusion.*. Ukr. J. Phys. 36 (1991), pp. 286–291.
[22] F. Hodaj, A.M. Gusak and P.J. Desre, *Effect of sharp concentration gradients on the nucleation of intermetallics in disordered solids: influence of the embryo shape*. Philos. Mag. A 77(6) (1998), pp. 1471–1479. doi:10.1080/01418619808214264.
[23] A.M. Gusak, F. Hodaj and A.O. Bogatyrev, *Kinetics of nucleation in the concentration gradient*. J. Phys.: Condens. Matter 13(12) (2001), pp. 2767. doi:10.1088/0953-8984/13/12/302.
[24] L.S. Darken, *Diffusion of carbon in austenite with a discontinuity in composition*. Trans. AIME 180 (1949), pp. 430–438.
[25] L.N. Paritskaya, *Kirkendall effect: dramatic history of discovery and developments*, in *Defect and Diffusion Forum*, Trans Tech Publications Ltd, 2006, Vol. 249, pp. 73–80. doi:10.4028/www.scientific.net/DDF.249.73.
[26] Y.S. Kaganovskii and L.N. Paritskaya. Metallofiz. Vol .4 (1982), p. 103.
[27] K.P. Gurov, A.M. Gusak, V.V. Kondrat'yev, M.V. Yarmolenko, *On the description of interdiffusion and Kirkendall effect in alloys with fine-grained structure*. THE PHYSICS OF METALS AND METALLOGRAPHY 6(#1) (1988), pp. 29–35.
[28] L. Klinger and E. Rabkin, *Theory of the Kirkendall effect during grain boundary interdiffusion*. Acta Mater. 59(4) (2011 Feb 1), pp. 1389–1399. doi:10.1016/j.actamat.2010.10.070.
[29] K.P. Gurov and A.M. Gusak, *A description of interdiffusion in alloys with an arbitrary capacity of vacancy sinks*. Fiz. Met. Metalloved 59(6) (1985), pp. 1062–1066.
[30] A.M. Gusak and M.V. Yarmolenko, *A simple way of describing the diffusion phase growth*. J. Appl. Phys. 73(10) (1993), pp. 4881–4884. doi:10.1063/1.353805.
[31] S.R. De Groot and P. Mazur. Non-equilibrium thermodynamics, 'North-Holland' (1962).
[32] P. Glansdorff and I. Prigogine, *Thermodynamic Theory of Structure, Stability and Fluctuations*, Wiley-Interscience, New York, 1971. doi:10.1002/bbpc.19720760520

Appendix

Appendix. Lateral interdiffusion along spherical interface i/B

Let us consider the flux balances along the interface in the case when the interface is not planar but instead has the shape of moving spherical cap with some curvature radius ρ_k

$$dl = \frac{dr}{\cos\theta} = \rho d\theta,\ \ r = \rho\sin\theta \ \ - \text{elementary geometry.}$$

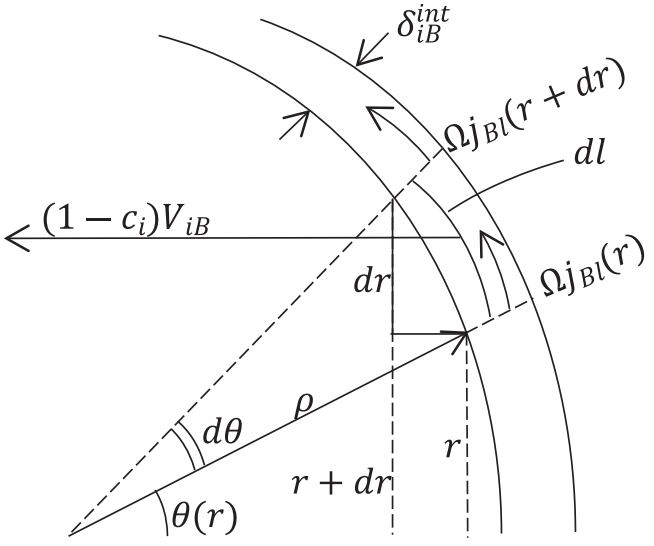

Fig. A1.1. Fluxes in-, out- and along the elementary volume at the interface i/B.

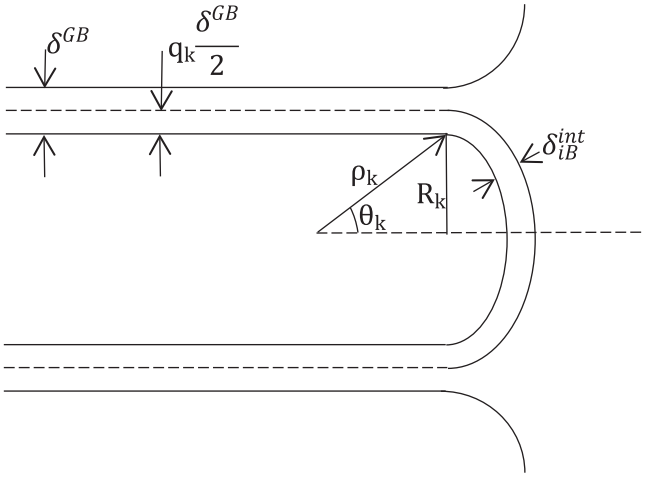

Fig. A1.2.

Flux balance in the reference frame of the moving interface I/B:

$$2\pi r\delta_{iB}^{int}\cdot\Omega j_l^{\perp}(r)-2\pi(r+dr)\cdot\delta_{iB}^{int}\cdot\Omega j_l^{\perp}(r+dr)+2\pi r\delta_{iB}^{int}(1-c_i)V_{iB}\sin\theta(r)$$

$$-2\pi(r+dr)\delta_{iB}^{int}(1-c_i)V_{iB}\sin\theta(r+dr)+(1-c_i)V_{iB}\cos\theta(r)\cdot 2\pi r dl=0 \qquad (A1.1)$$

$$d\{[\Omega j_l^{\perp}+(1-c_i)V_{iB}\sin\theta]\cdot r\}=\frac{1}{\delta_{iB}^{int}}(1-c_i)V_{iB}\cdot r dr$$

$$\Omega j_l^{\perp}(r)=\frac{(1-c_i)V_{iB}}{2\delta_{iB}^{int}}\cdot(r-2\delta_{iB}^{int}\sin\theta(r)) \qquad (A1.2)$$

Almost everywhere $r\gg 2\delta_{iB}^{int}\sin\theta$ =>

$$\Omega j_l^{\perp}(r)\cong\frac{(1-c_i)V_{iB}}{2\delta_{iB}^{int}}\cdot r, \qquad \Omega j_l^{\perp}(R_k)\cong\frac{(1-c_i)V_{iB}}{2\delta_{iB}^{int}}\cdot R_k \qquad (A1.3)$$

Let us translate Equation (A1.3) into the equation for diffusion potential:

$$\Omega j_l=-\tilde{L}_{iB}^{int}\frac{\partial\tilde{\mu}}{\partial l}=-\tilde{L}_{iB}^{int}\frac{\partial\tilde{\mu}}{\partial r}\cos\theta=\frac{(1-c_i)V_{iB}}{2\delta_{iB}^{int}}\cdot r, \qquad (A1.4)$$

$$d\ddot{A}=-\frac{(1-c_i)V_{iB}}{2\delta_{iB}^{int}}\cdot r\frac{1}{\cos\theta}dr=-\frac{(1-c_i)V_{iB}}{2\delta_{iB}^{int}}\rho^2\sin\theta d\theta, \qquad (A1.5)$$

$$\Delta\widetilde{\mu_{iB}}=\tilde{\mu}(0)-\tilde{\mu}(R_k)=\frac{(1-c_i)V_{iB}}{2\delta_{iB}^{int}}\frac{R_k^2}{\sin^2\theta_k}(1-\cos\theta_k)=\frac{(1-c_i)V_{iB}}{4\delta_{iB}^{int}}\frac{R_k^2}{\cos^2\left(\frac{\theta_k}{2}\right)}. \qquad (A1.6)$$

Now we use the continuity equation, to link the longitudinal flux along grain-boundaries and lateral fluxes along interfaces:

$$-2\pi R_k\frac{\delta^{GB}}{2}q_k\Omega j_{GB}^{\parallel}=2\pi R_k\delta_{iB}^{int}\Omega j_l^{\perp}(R_k).$$

Here q_k is a factor taking into account the dispersion of lateral radii and corresponding dispersion of lateral fluxes.

$$q_k\left(\tilde{L}^{GB}\frac{\Delta\tilde{\mu}^{\parallel}}{\Delta x}\right)=\frac{2\delta_{iB}^{int}}{\delta^{GB}}\frac{(1-c_i)V_{iB}}{2\delta_{iB}^{int}}R_k => q_k=QR_k$$

$$\sum_k 2\pi R_k\frac{\delta^{GB}}{2}q_k=\sum_k 2\pi R_k\frac{\delta^{GB}}{2}\equiv A^{GB}, \quad Q=\frac{\sum_k R_k}{\sum_k R_k^2}=\frac{\langle R\rangle}{\langle R^2\rangle}$$

$$V_{iB}=\frac{\delta^{GB}\langle R\rangle}{\langle R^2\rangle}\cdot\frac{1}{1-c_i}\tilde{L}^{GB}\frac{\Delta\tilde{\mu}^{\parallel}}{\Delta x}, \quad V_{Ai}=-\frac{\delta^{GB}\langle R\rangle}{\langle R^2\rangle}\cdot\frac{1}{c_i}\tilde{L}^{GB}\frac{\Delta\tilde{\mu}^{\parallel}}{\Delta x}$$

$$\frac{d\Delta x}{dt}=\frac{const}{\langle R^2\rangle/\langle R\rangle(\Delta x+p\langle R^2\rangle/\langle R\rangle)}$$